

Reactive Simulations of Silica Functionalization with Aromatic Hydrocarbons

Published as part of *Langmuir* virtual special issue “2023 Pioneers in Applied and Fundamental Interfacial Chemistry: Nicholas D. Spencer”.

Sergio Romero Garcia, Yerzhan S. Zholdassov, Adam B. Braunschweig, and Ashlie Martini*



Cite This: *Langmuir* 2024, 40, 561–567



Read Online

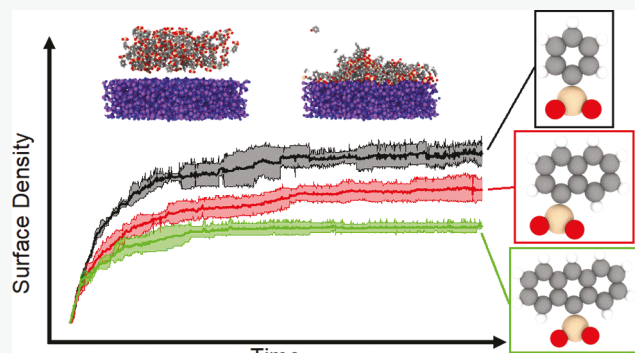
ACCESS |

Metrics & More

Article Recommendations

Supporting Information

ABSTRACT: Reactive molecular dynamics simulations are used to model the covalent functionalization of amorphous silica with aromatic hydrocarbons. Simulations show that the surface density of silanol-terminated phenyl, naphthyl, and anthracenyl molecules is lower than the maximum value calculated based on molecule geometry, and the simulation densities decrease faster with the number of aromatic rings than the geometric densities. The trends are analyzed in terms of the surface–silanol bonding configurations, tilt angles, local conformational ordering, and aggregation of surface-bound molecules under steady-state conditions. Results show that the surface density is affected by both the size and symmetry of the aromatic hydrocarbons. The correlations among bonding, orientation, and surface density identified here may guide the selection or design of molecules for functionalized surfaces.



INTRODUCTION

Modification of silica surfaces with organic molecules is important for the development of medical, electronic, and pharmaceutical applications. Chemical bonds that form between a silica substrate and organic molecules modify the chemical and physical properties of the surface.¹ This opens the possibility to control or tailor properties such as friction,² biocompatibility,³ and polarity⁴ to a specific application. Examples include the functionalization of atomic force microscope tips to improve their useful life,⁵ design of biocompatible amorphous silica⁶ in drug delivery systems and implant applications⁷ to treat osteoporotic fractures⁸ and bone tumors or infections,⁹ development of sensors for detecting biological analytes,¹⁰ and creation of stimuli-responsive surfaces.¹¹

Many different organic molecules have been immobilized on silica through the formation of new covalent bonds with the surface.¹² Among these, aromatic hydrocarbons (AHs) have been used in solution-based and mechanochemically driven pericyclic reactions¹³ and proposed for applications in organic electronic devices.¹⁴ AHs are composed of aromatic carbon rings, with those in the acene group made up of linearly bonded rings. In solution-based chemistry, functionalizing silica with AHs is possible at room temperature.¹² However, to further the development of AH silica functionalization as a predictable method to control surface properties, the

mechanisms underlying chemical bond formation between the AH molecules and the silica surface must be understood.

Importantly, chemical bonding affects the density of organic molecules on the surface, which, in turn, determines the properties of the functionalized surface.¹⁵ Observations of the change in contact angle of aromatic-modified substrates suggested that surface density is affected by the orientation and size of the deposited molecules.¹⁶ Studies of the surface properties of heterogeneous polycyclic AH clusters¹⁷ in soot showed that the surface densities of carbon atoms in solid-like configurations were affected by the structure of the surface-bound molecules, with smaller molecules, such as pyrene, contributing significantly to the surface density. Further, previous experiments showed that the adsorption of organic molecules with different functional groups on silica can be favored by molecular flexibility and good steric access of the adsorption active groups to the silica surface.¹⁸

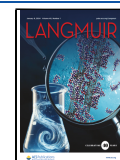
Surface density can be estimated based on the geometry of a given molecule or measured using a quartz crystal micro-

Received: September 16, 2023

Revised: November 2, 2023

Accepted: December 5, 2023

Published: December 19, 2023



balance (QCM).^{19,20} Specific to the QCM method, by estimating the monolayer mass of the deposited molecules, it is possible to measure surface density. However, this method does not provide insight into the underlying chemical and physical processes and, particularly, the effect of the structures of the deposited molecules. Computational methods can provide complementary information about molecules and surface interactions at the atomic level. Some studies have used *ab initio* methods^{7,21} for this purpose. However, the scaling of quantum calculations [i.e., $O(N_{\text{electrons}}^3)$] makes such calculations unsuitable for modeling systems larger than a thousand atoms. In contrast, classical molecular dynamics (MD) simulations based on empirical potentials are more efficient as they scale with the number of atoms in the system [i.e., $O(N_{\text{atoms}})$].

The development of empirical potentials that model chemical reactions, such as ReaxFF,²² has made it possible to observe bond formation in a dynamic simulation. The ReaxFF potential has been shown to accurately describe the geometry, stability, and chemical bonding of conjugate, nonconjugate, and radical-containing compounds.²³ Relevant to our current investigation, ReaxFF simulations have been used to study the formation of alkylsilane self-assembled monolayers (SAM) on silica²⁴ and shear-activated oxidative chemisorption and oligomerization of cyclic hydrocarbons on amorphous silica.^{25,26} Simulations of the functionalization of crystalline silicon surfaces with alkyl radicals were able to accurately reproduce surface densities measured experimentally.²⁷

In our previous work,²⁸ a method to simulate the functionalization of amorphous silica with 9-anthracenyl trimethoxysilane was developed to corroborate the surface density obtained from experimental solution-based depositions with good agreement between experiments and simulations. In experiments, the packing of AH monolayers is controlled by using a closed saturated solvent environment²⁹ (e.g., PhMe) that promotes reactions between the hydroxylated substrate and the silane–methyl-terminated AH molecule. This opens oxygen-reactive sites for the silanol termination on the AH molecules to form covalent bonds with the surface. To focus on the covalent bonding of molecules to the substrate and improve simulation times, the previous simulations were performed using a model system in which the silica was dehydroxylated and the depositing molecules were AH-terminated by a dehydroxylated silanol group, subsequently termed simply silanols in this article. These simulations showed the time evolution of surface density, where the simulated steady-state value was in agreement with the density measured using QCM.²⁸ However, the study did not provide insight into the effect of the silanol structure on surface density, which is key for the selection of chemical species for surface functionalization for a specific application.

Here, we expand on our previous work by using reactive MD simulations to understand the effect of molecular structures on the covalent functionalization of amorphous silica with silanols and specifically on surface density. We model the condensation reactions between silica and three silanols with different numbers of aromatic rings at three different temperatures. We compare simulation-calculated densities with those estimated by using simple geometric models based on van der Waals radii. Then, we analyze surface densities in terms of the type and number of covalent bonds formed with the amorphous silica and the orientation and ordering of the silanols, revealing

correlations between surface density and local conformational ordering of the silanols on the silica surface.

MATERIALS AND METHODS

The model system comprised a dehydroxylated silica substrate and AHs terminated by a dehydroxylated silanol group (silanols). This simplified model mimics the last step of reactions reported in our previous experimental study.²⁸ Specifically, in the experiments, a silica substrate was immersed in a PhMe solution containing 9-anthracenyl trimethoxysilane to initiate reactions between the methyl termination of the AHs and the hydroxyl groups on the substrate surface. The reaction was assumed to proceed through initial steps to form dangling bonds on the substrate and AHs, leading to chemical bonding between $\text{Si}_{\text{substrate}}$ and O_{AH} . Therefore, we modeled only the last step, i.e., the reaction between dehydroxylated silica and dehydroxylated silanols, to maximize the number of reactions of interest within the size and time-scale limitations of the reactive MD method.

The amorphous SiO_2 was generated from a cristobalite SiO_2 crystal structure³⁰ that was heated (5000 K) and fast quenched (300 K) in a simulation box with periodic boundary conditions in all directions and dimensions $5.6 \times 6.0 \times 2.1 \text{ nm}$ (x , y , and z). The resulting amorphous structure exhibited $\text{Si}=\text{O}$, $\text{O}=\text{O}$, and $\text{Si}=\text{Si}$ peaks and distances characterized by radial distribution functions (RDFs) (Supporting Information Figure S1) that showed good agreement with values reported in literature for amorphous SiO_2 thin films.³¹ Then, the dimensions of the box were extended to $5.6 \times 6.0 \times 5.5 \text{ nm}$ (x , y , and z) to create a surface. The density of accessible dangling bonds on the equilibrated substrate surface before deposition was calculated to be 4.55 nm^{-2} with 153 open sites available for reaction.

Three silanols were modeled, phenyl, naphthyl, and anthracenyl, as shown in Figure 1A. The silanols were designed with the Avogadro

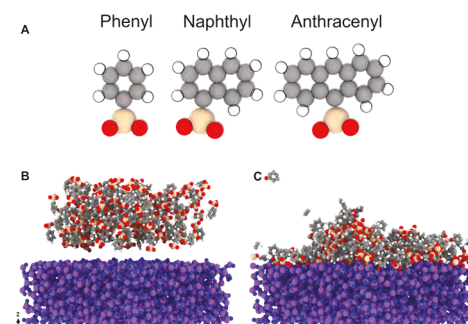


Figure 1. (A) Schematic representations of the AHs used as reactants in the simulations. Representative side-view snapshots of the model system with phenyl (B) before and (C) after covalent functionalization. Sphere colors correspond to gray, carbon; white, hydrogen; tan, silicon in the silanols; purple, silicone in the silica; red, oxygen in the silanols; and blue, oxygen in the silica.

chemical editor³² and then placed randomly into the simulation box at a distance of at least 0.5 nm from the silica surface using PACKMOL.³³ The characterization of functionalized surfaces in the corresponding previous experiments suggested complete surface coverage.²⁸ Based on this, the number of silanols per simulation, 150, was determined as the approximate number needed to ensure full surface coverage within the short time-scale of the simulations. After this stage, the boundary conditions were periodic in x and y , while the z boundaries were fixed. The bottommost atoms in the silica slab were fixed during the simulation, and a repulsive wall was used at the top of the simulation box to prevent silanols from escaping.

Reactive MD simulations were performed using the large-scale atomic/molecular massively parallel simulator (LAMMPS)³⁴ package. Atomic interactions were modeled with a time step of 0.1 fs using the ReaxFF potential for H/C/O/Si ³⁵ parameterized to maintain the thermal stability of $\text{C}-\text{Si}$ bonds in silicon surfaces functionalized with

organic molecules. Initial atom velocities were given by a Gaussian distribution at three different temperatures (300, 400, and 500 K). Simulations were run using the NVT ensemble (constant number of particles, volume, and temperature) using a Nosé–Hoover³⁶ thermostat with a damping parameter of 40 fs.

The simulations were run at each of the three temperatures for at least 0.2 ns, which was determined to be enough time for the surface reactions to reach a steady state, as shown in Supporting Information Figure S2. Snapshots of a representative model system before and after a dynamic simulation are shown in Figure 1B,C. Each simulation case was replicated three times by using different random seed values for the initial atom velocities, such that the repeat simulations were independent. Trajectory information was output every 5 ps, and the bond table from ReaxFF that tracks the strength and number of covalent bonds was output every 0.2 ps. Visualization and analysis of atomic chemisorption from simulated data were done in the OVITO³⁷ open-visualization tool and custom scripts written in Python.

RESULTS AND DISCUSSION

During the simulations, chemical bonds were formed between silicon in the silanols and oxygen on the silica surface. The number of silanols chemically bound to the surface was tracked (based on the formation of Si_{silanol}–O_{silica} bonds) and surface density was calculated from the number of surface-bound silanols divided by the silica surface area (32.9 nm²). The time evolution of the surface density at each temperature for phenyl, naphthyl, and anthracenyl is shown in Figure 2A–C,

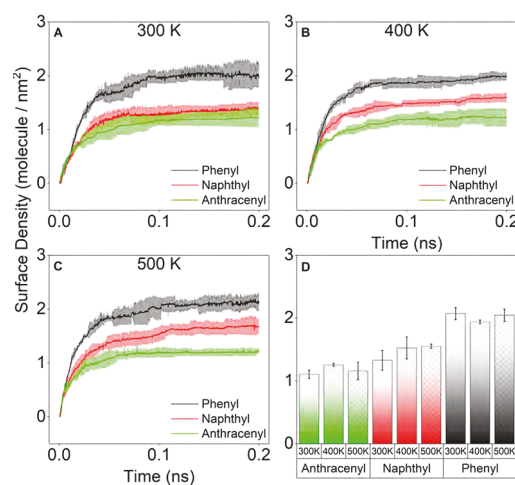


Figure 2. Time evolution of the surface density for phenyl, naphthyl, and anthracenyl chemisorbed on an amorphous silica surface from simulations at (A) 300, (B) 400, and (C) 500 K. For each data set, the dark line is the mean and the shaded region is the standard deviation of three independent simulations. (D) Steady-state surface density for each case is averaged over the last 0.1 ns of the simulations, where error bars reflect the standard deviation.

respectively. Bond formation occurred as soon as the simulation began, and the surface density increased rapidly during the first 0.05 ns in all cases. The density reached a steady-state value after about 0.1 ns. At the end of the simulation, the silica surface was covered by a monolayer of chemically bound silanols, e.g., Figure 1C. The trajectories of the silanols were also tracked, showing that silanol movement on the surface was negligible after a steady state was reached (Figures S4 and S5). Therefore, subsequent analyses focused on characterizing the bonding, conformation, and orientation of the surface-bound silanols between 0.1 and 0.2 ns.

The steady-state surface density for each silanol and temperature averaged over three independent simulations are reported in Figure 2D. The results show that temperature did not have a statistically significant effect on surface density but the densities were very different for the three different silanols. Therefore, subsequent analyses focused on the silanols and included data from simulations at all three temperatures. The average steady-state surface densities were 2.06 ± 0.12 , 1.38 ± 0.15 , and 1.15 ± 0.09 nm⁻² for phenyl, naphthyl, and anthracenyl, respectively. The value for anthracenyl is comparable to the surface density previously measured using QCM of 1.12 ± 0.13 nm⁻².²⁸ Further, the trend with respect to the three silanols is consistent with the expectation that the larger silanols should occupy more surface area and therefore have a lower density.

The maximum possible density for each silanol can be estimated based on the size of the molecules. Specifically, the van der Waals areas of the molecules³⁸ in the *xy* plane (visual representations in Supporting Information Figure S3) were calculated to be 0.438, 0.582, and 0.720 nm², corresponding to maximum surface densities of 2.28, 1.71, and 1.38 nm⁻² for phenyl, naphthyl, and anthracenyl, respectively. These values as well as the densities obtained from simulations and reported from experiments are given in Table 1. The simulation and

Table 1. Summary of Surface Density Values Estimated Based on Molecule Geometry, Reactive MD Simulations, and Previous QCM Measurements²⁸

method	surface density (nm ⁻²)		
	phenyl	naphthyl	anthracenyl
geometric maximum	2.28	1.71	1.38
MD simulations	2.06 ± 0.12	1.38 ± 0.15	1.15 ± 0.09
QCM experiments			1.12 ± 0.13

experimental densities are lower than the maximum based on molecule geometry, which is reasonable since the maximum value assumes that the silanols are ideally conformationally ordered, which is not expected to be the case in practice. The biggest difference between simulated and geometric density is for naphthyl. Also, the simulation densities decrease faster with an increasing number of aromatic rings than the geometric densities. For example, the ratio of the theoretical densities of anthracenyl and phenyl is 1.65 but was found to be 1.79 ± 0.18 in the simulations.

Analysis of anthracenyl chemisorption studied previously²⁸ showed that there are three types of bonding configurations possible, depending on how many silicon–oxygen bonds are formed, as illustrated in the close-up snapshots in Figure 3A–C. Figure 3D shows the distribution of bonding configurations for the surface-bound silanols, including data from all three simulated temperatures. The bond type distribution shows that the likelihood of a given configuration decreased with the number of bonds. Specifically, for all silanols, one oxygen bond (1-O) was the most common, and the least observed bonding configuration was three oxygen (3-O) atoms. However, the statistical difference between 1-O and 2-O was the smallest for naphthyl, and the average percentage of 3-O was the largest for this silanol.

Since the orientation of the surface-bound silanols can play a significant role in the properties of functionalized silica surfaces, the angle of tilt of the silanol with respect to the surface was analyzed. The tilt angle θ was defined as the angle

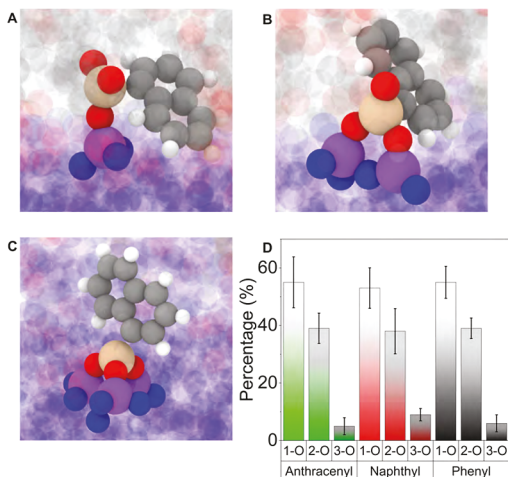


Figure 3. Close-up snapshots of the three possible bonding configurations between a silanol and the silica substrate that differ based on the number of $\text{Si}_{\text{silanol}}-\text{O}_{\text{silica}}$ bonds, shown using naphthyl as a reference: (A) one bond (1-O), (B) two bonds (2-O), and (C) three bonds (3-O). Spheres representing atoms other than those in the representative silanols of interest are faded. (D) Distribution of the number of bonds between Si in the substrate and O in the silanol averaged over the three simulations at three temperatures for each silanol as a percentage of the total number of silanols in the system. The error bars represent the standard deviation.

between the plane of the ring(s) in the silanol and the direction normal to the silica surface, as shown in Figure 4A.

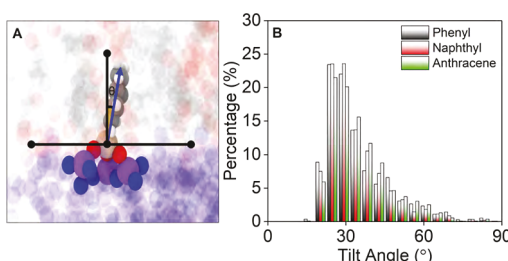


Figure 4. (A) Representative snapshot of phenyl showing the definition of the angle used to quantify the tilt of the silanol with respect to the surface-normal direction. Spheres representing atoms other than those in the representative silanol of interest are faded. (B) Distribution of tilt angles from all observed bonds and all temperatures and simulations between 0.1 and 0.2 ns of simulation time. Only slight differences between phenyl, naphthyl, and anthracenyl are observed, but smaller angles are preferred for the smaller silanols.

The angle was calculated for each silanol bonded to the substrate using data from 0.1 to 0.2 ns of simulation time. The distributions of tilt angles in Figure 4B are positively skewed where the highest angle probability is 28.4° for all three silanols (distribution modes are 27.9 ± 0.5 , 28.7 ± 0.6 , and $30.3 \pm 0.8^\circ$ for phenyl, naphthyl, and anthracenyl, respectively). This is consistent with the range of angles for SAM on amorphous silica, which have been reported to be 16° at full coverage³⁹ and as low as 30° for low coverage.⁴⁰ The highest angle probability of 28° for silanols in our study is at the upper end of the range reported for SAMs, consistent with the fact that our surface densities are below the geometric value (Table 1). Lastly, although the distributions are very similar for all three silanols, there are more small angles for the phenyl. This is

consistent with a previous simulation-based study⁴¹ of alkanethiol SAMs that reported tilt angle increased with chain length.

Another factor that can affect the surface density of AHs is the orientation of molecules with respect to each other. Figure 5A–C shows two point vector representations of the surface-bound silanols in the xy plane for representative simulations. The vector is defined from the positions of the two edge carbon atoms on the long axis of the silanol, as shown in Figure 5 insets. The line corresponding to each vector is colored based on its angle with respect to the x -axis; the x -axis is an arbitrary direction, but if the silanols are conformationally ordered, there will be more lines in Figure 5A–C with similar colors. This qualitative analysis shows some evidence of local ordering, but clearly the silanols are not ordered into the closest packed configuration assumed in the geometric density calculations (Figure S3). This may be correlated to the preferential 1-O bonding exhibited by all three silanols in Figure 3D since fewer chemical bonds enable greater flexibility and rotation ability.

Next, we quantified the local ordering using RDFs⁴¹ of the distance between Si atoms in the surface-bound silanols for all the frames between 0.1 and 0.2 ns. The results for all simulations and temperatures are shown in Figure 5D–F. If the silanols were ordered in their closest packed configuration, the smallest distance between silanols would be ≈ 0.3 nm. This is approximately where the first peak is seen in the RDFs in all three cases. However, there are also differences among the three silanols. Particularly, the first peak is the broadest and shortest for phenyl, indicating these silanols are the least conformationally ordered. Less conformational ordering is associated with a larger available volume for conformational changes, consistent with the smaller tilt angles for phenyl in Figure 4B.

The RDF peaks at farther distances reflect a longer-range ordering of the silanols. Interestingly, for phenyl and anthracenyl, there are distinct peaks around 0.40, 0.47, and 0.55 nm, associated with the preferred orientations of adjacent chemisorbed species. However, for naphthyl, the RDF peaks are broader and less distinct, indicating a less long-range order.

The naphthyl also had the least distinction between the different bonding configurations in Figure 3D and the largest difference between the simulated and estimated surface densities in Table 1. The difference between naphthyl and the other two silanols is symmetry, with only naphthyl being asymmetric relative to the silicon atom. These results show that asymmetry decreases long-range order, which, in turn, decreases the achievable surface density relative to the maximum possible value.

Finally, surface density may be affected by the interaction and bonding between silanols, resulting in aggregates.⁴² An example is shown in Figure 6A, where two naphthyl molecules associate via an oxygen bond. This behavior was analyzed for all three silanols by calculating the distributions of aggregate size (e.g., 1-silanol, 2-silanol, 3-silanol, etc.) during the steady state, as shown in Figure 6B. The most commonly observed configuration is 1 silanol, meaning it is not aggregated. However, all three molecules form multiple dimers and trimers as well as even larger aggregates. Comparing the three silanols, anthracenyl has the fewest and smallest aggregates, while phenyl has the most and largest aggregates. Since the association reactions always occur via an Si–O–Si bond, the trend observed in the aggregation results can be associated

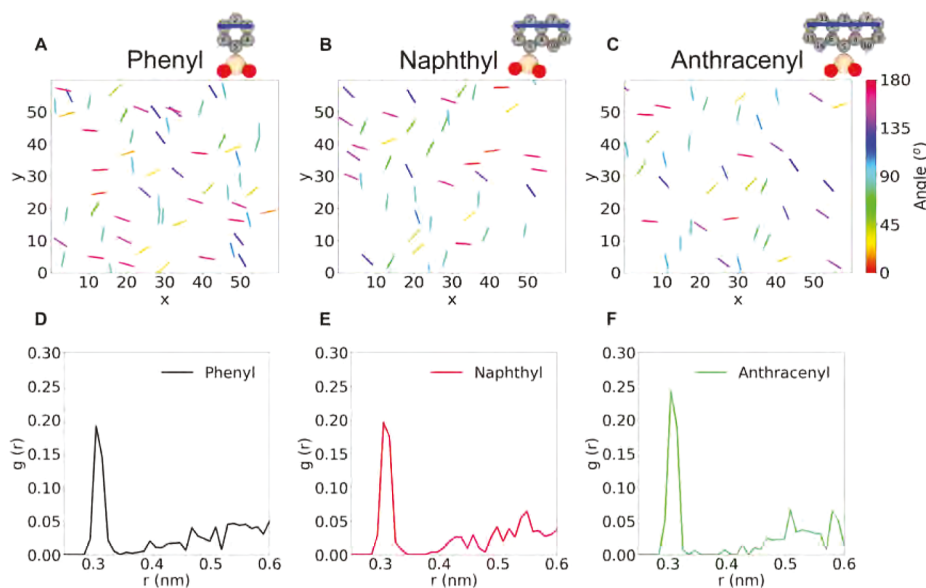


Figure 5. Two-point vector representations of the silanol in the xy plane from representative simulations of (A) phenyl, (B) naphthyl, and (C) anthracenyl. The two point coordinates are taken from the edge carbons on the long axis of the silanol, as shown in the insets. The x - and y -axes are scaled by the total length of the simulation box in each direction. RDFs of the distance between Si atoms in (D) phenyl, (E) naphthyl, and (F) anthracenyl were obtained for all simulations.

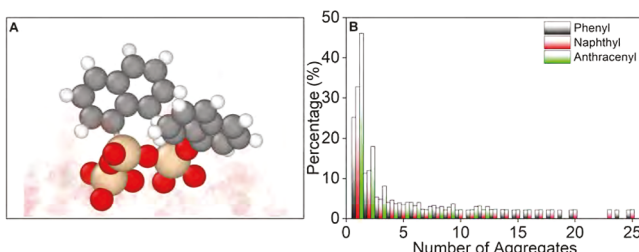


Figure 6. (A) Representative snapshot of a two-naphthol aggregate. (B) Distributions of aggregate size (quantified by the number of bonded silanols) for each silanol calculated from trajectory data between 0.1 and 0.2 ns.

with molecular size and surface density, where larger silanols are further apart and less likely to aggregate.

CONCLUSIONS

Reactive simulations were used to study the covalent functionalization of amorphous silica with silanol AHs. Surface density increased with decreasing molecular size, consistent with the maximum densities estimated from molecule geometry in a closest-packed configuration. The simulation densities were smaller than the estimated maximum values, and the biggest difference between simulation and estimation was observed for naphthyl. Three possible chemical bonding configurations were observed, and it was shown that all three silanols preferentially formed fewer covalent bonds, facilitating bending or rotation. Tilt angles were also calculated and shown to be smaller for the smaller molecules. Local conformational ordering, analyzed qualitatively and quantitatively, was found to increase with molecule size. However, the least long-range order was exhibited by the asymmetric naphthyl silanol, a result that was correlated to the larger difference between the simulation and the estimated surface density. Finally, the analysis of the aggregation of surface-bound species showed that smaller size and higher density were also associated with

the formation of more and larger aggregates. These results show that both size and symmetry affect the surface density achievable in the covalent functionalization of surfaces with silanol AHs. Future work using ab initio calculations may corroborate these findings and provide further insight into the structure-bonding relationship. Generally, these simulation-based approaches can inform our understanding of how molecular structure affects surface density, which can guide the selection or design of molecules to achieve an ideal surface density and, in turn, ideal properties for a specific surface or application.

ASSOCIATED CONTENT

Supporting Information

The Supporting Information is available free of charge at <https://pubs.acs.org/doi/10.1021/acs.langmuir.3c02785>.

RDFs for the substrate Si–O, O–O, and Si–Si atom pairs before and after the amorphization step; surface density calculations from extended simulation run times for selected systems; schematic representation of the theoretical surface density calculations for each molecule type; and representative snapshots of silanol trajectories and the mean square displacement of the silanol over time at different temperatures (PDF)

AUTHOR INFORMATION

Corresponding Author

Ashlie Martini – Department of Mechanical Engineering, University of California Merced, Merced, California 95343, United States; orcid.org/0000-0003-2017-6081; Phone: +1 (209) 228-2354; Email: amartini@ucmerced.edu

Authors

Sergio Romero Garcia – Department of Materials and Biomaterials Science and Engineering, University of

California Merced, Merced, California 95343, United States;
orcid.org/0000-0002-4891-4763

Yerzhan S. Zholdassov – The Advanced Science Research Center at the Graduate Center of the City University of New York, New York, New York 10031, United States; Department of Chemistry, Hunter College, New York, New York 10065, United States; The Ph.D. Program in Chemistry, Graduate Center of the City University of New York, New York, New York 10016, United States

Adam B. Braunschweig – The Advanced Science Research Center at the Graduate Center of the City University of New York, New York, New York 10031, United States; Department of Chemistry, Hunter College, New York, New York 10065, United States; The Ph.D. Program in Chemistry, Graduate Center of the City University of New York, New York, New York 10016, United States

Complete contact information is available at:
<https://pubs.acs.org/10.1021/acs.langmuir.3c02785>

Notes

The authors declare no competing financial interest.

ACKNOWLEDGMENTS

This work was supported by the National Science Foundation (NSF) Center for the Mechanical Control of Chemistry (CMCC), CHE-2023644 and CHE-2303044. The CMCC is part of the NSF Centers for Chemical Innovation Program. Simulations were run on resources provided by the ACCESS advanced computing and data resource supported by the NSF.

REFERENCES

- (1) Barth, J. V.; Costantini, G.; Kern, K. Engineering atomic and molecular nanostructures at surfaces. *Nature* **2005**, *437*, 671–679.
- (2) Sui, T.; Song, B.; Wen, Y.-H.; Zhang, F. Bifunctional hairy silica nanoparticles as high-performance additives for lubricant. *Sci. Rep.* **2016**, *6*, 22696.
- (3) Zhang, S.; Niu, H.; Zhang, Y.; Liu, J.; Shi, Y.; Zhang, X.; Cai, Y. Biocompatible phosphatidylcholine bilayer coated on magnetic nanoparticles and their application in the extraction of several polycyclic aromatic hydrocarbons from environmental water and milk samples. *J. Chromatogr. A* **2012**, *1238*, 38–45.
- (4) Filler, M. A.; Bent, S. F. The surface as molecular reagent: organic chemistry at the semiconductor interface. *Prog. Surf. Sci.* **2003**, *73*, 1–56.
- (5) Berman, D.; Krim, J. Surface science, MEMS and NEMS: Progress and opportunities for surface science research performed on, or by, microdevices. *Prog. Surf. Sci.* **2013**, *88*, 171–211.
- (6) Lai, C.-Y.; Trewyn, B. G.; Jeftinija, D. M.; Jeftinija, K.; Xu, S.; Jeftinija, S.; Lin, V. S.-Y. A mesoporous silica nanosphere-based carrier system with chemically removable CdS nanoparticle caps for stimuli-responsive controlled release of neurotransmitters and drug molecules. *J. Am. Chem. Soc.* **2003**, *125*, 4451–4459.
- (7) Corno, M.; Delle Piane, M.; Choquet, P.; Ugliengo, P. Models for biomedical interfaces: a computational study of quinone-functionalized amorphous silica surface features. *Phys. Chem. Chem. Phys.* **2017**, *19*, 7793–7806.
- (8) Ilyas, A.; Odatsu, T.; Shah, A.; Monte, F.; Kim, H. K. W.; Kramer, P.; Aswath, P. B.; Varanasi, V. G. Amorphous Silica: A New Antioxidant Role for Rapid Critical-Sized Bone Defect Healing. *Adv. Healthcare Mater.* **2016**, *5*, 2199–2213.
- (9) Sayed, E.; Haj-Ahmad, R.; Ruparelia, K.; Arshad, M. S.; Chang, M.-W.; Ahmad, Z. Porous Inorganic Drug Delivery Systems-a Review. *AAPS PharmSciTech* **2017**, *18*, 1507–1525.
- (10) Valles, D. J.; Zholdassov, Y. S.; Korpanty, J.; Uddin, S.; Naeem, Y.; Mootoo, D. R.; Gianneschi, N. C.; Braunschweig, A. B. Glycopolymers Microarrays with Sub-Femtomolar Avidity for Glycan Binding Proteins Prepared by Grafted-To/Grafted-From Photopolymerizations. *Angew. Chem., Int. Ed. Engl.* **2021**, *60*, 20350–20357.
- (11) Zholdassov, Y. S.; Valles, D. J.; Uddin, S.; Korpanty, J.; Gianneschi, N. C.; Braunschweig, A. B. Orthogonal Images Concealed Within a Responsive 6-Dimensional Hypersurface. *Adv. Mater.* **2021**, *33*, No. e2100803.
- (12) Rimola, A.; Costa, D.; Sodupe, M.; Lambert, J.-F.; Ugliengo, P. Silica surface features and their role in the adsorption of biomolecules: computational modeling and experiments. *Chem. Rev.* **2013**, *113*, 4216–4313.
- (13) Sulkannan, A. R.; Sung, J.; Robb, M. J.; Moore, J. S.; Sottos, N. R.; Liu, G. Y. Spatially Selective and Density-Controlled Activation of Interfacial Mechanophores. *J. Am. Chem. Soc.* **2019**, *141*, 4080–4085.
- (14) Tao, F. *Functionalization of Semiconductor Surfaces*; Wiley: Hoboken, NJ, 2012.
- (15) Veerbeek, J.; Huskens, J. Applications of monolayer-functionalized H-terminated silicon surfaces: A review. *Small Methods* **2017**, *1*, 1700072.
- (16) Hong, Y.; Chen, W.; Fang, H.; Zuo, B.; Yuan, Y.; Zhang, L.; Wang, X. Regulation of the Interfacial Effects of Thin Polystyrene Films by Changing the Aromatic Group Structure on Substrate Surfaces. *J. Phys. Chem. C* **2019**, *123*, 19715–19724.
- (17) Bowal, K.; Pascazio, L.; Wang, H.; Chen, D.; Kraft, M. Surface properties of heterogeneous polycyclic aromatic hydrocarbon clusters. *Proc. Combust. Inst.* **2021**, *38*, 1115–1123.
- (18) Diaz, L.; Liauw, C. M.; Edge, M.; Allen, N. S.; McMahon, A.; Rhodes, N. Investigation of factors affecting the adsorption of functional molecules onto gel silicas. 1. Flow microcalorimetry and infrared spectroscopy. *J. Colloid Interface Sci.* **2005**, *287*, 379–387.
- (19) Stålgren, J. J. R.; Eriksson, J.; Boschkova, K. A comparative study of surfactant adsorption on model surfaces using the quartz crystal microbalance and the ellipsometer. *J. Colloid Interface Sci.* **2002**, *253*, 190–195.
- (20) Sauerbrey, G. Verwendung von Schwingquarzen zur Wägung dünner Schichten und zur Mikrowägung. *Z. Phys.* **1959**, *155*, 206–222.
- (21) Leftwich, T. R.; Madachik, M. R.; Teplyakov, A. V. Dehydrative cyclocondensation reactions on hydrogen-terminated Si(100) and Si(111): An ex situ tool for the modification of semiconductor surfaces. *J. Am. Chem. Soc.* **2008**, *130*, 16216–16223.
- (22) van Duin, A. C. T.; Dasgupta, S.; Lorant, F.; Goddard, W. A. ReaxFF: A Reactive Force Field for Hydrocarbons. *J. Phys. Chem. A* **2001**, *105*, 9396–9409.
- (23) Han, Y.; Jiang, D.; Zhang, J.; Li, W.; Gan, Z.; Gu, J. Development, applications and challenges of ReaxFF reactive force field in molecular simulations. *Front. Chem. Eng.* **2016**, *10*, 16–38.
- (24) Black, J. E.; Iacovella, C. R.; Cummings, P. T.; McCabe, C. Molecular dynamics study of alkylsilane monolayers on realistic amorphous silica surfaces. *Langmuir* **2015**, *31*, 3086–3093.
- (25) Bhuiyan, F. H.; Kim, S. H.; Martini, A. Reactive molecular dynamics simulations of thermal and shear-driven oligomerization. *Appl. Surf. Sci.* **2022**, *591*, 153209.
- (26) Bhuiyan, F. H.; Li, Y.-S.; Kim, S. H.; Martini, A. Shear-activated chemisorption and association of cyclic organic molecules. *Faraday Discuss.* **2023**, *241*, 194–205.
- (27) Soria, F. A.; Zhang, W.; Paredes-Olivera, P. A.; Van Duin, A. C. T.; Patrito, E. M. Si/C/H ReaxFF Reactive Potential for Silicon Surfaces Grafted with Organic Molecules. *J. Phys. Chem. C* **2018**, *122*, 23515–23527.
- (28) Zholdassov, Y. S.; Yuan, L.; Garcia, S. R.; Kwok, R. W.; Boscoboinik, A.; Valles, D. J.; Marianski, M.; Martini, A.; Carpick, R. W.; Braunschweig, A. B. Acceleration of Diels-Alder reactions by mechanical distortion. *Science* **2023**, *380*, 1053–1058.
- (29) Huang, C.; Katz, H. E.; West, J. E. Solution-processed organic field-effect transistors and unipolar inverters using self-assembled interface dipoles on gate dielectrics. *Langmuir* **2007**, *23*, 13223–13231.

(30) Gutiérrez Moreno, J. J.; Pan, K.; Wang, Y.; Li, W. Computational Study of APTES Surface Functionalization of Diatom-like Amorphous SiO₂ Surfaces for Heavy Metal Adsorption. *Langmuir* **2020**, *36*, 5680–5689.

(31) Zhu, W.; Zheng, G.; Cao, S.; He, H. Thermal conductivity of amorphous SiO₂ thin film: A molecular dynamics study. *Sci. Rep.* **2018**, *8*, 10537.

(32) Hanwell, M. D.; Curtis, D. E.; Lonie, D. C.; Vandermeersch, T.; Zurek, E.; Hutchison, G. R. Avogadro: an advanced semantic chemical editor, visualization, and analysis platform. *J. Cheminform.* **2012**, *4*, 17.

(33) Martínez, L.; Andrade, R.; Birgin, E. G.; Martínez, J. M. PACKMOL: a package for building initial configurations for molecular dynamics simulations. *J. Comput. Chem.* **2009**, *30*, 2157–2164.

(34) Plimpton, S. Fast Parallel Algorithms for Short-Range Molecular Dynamics. *J. Comput. Phys.* **1995**, *117*, 1–19.

(35) Soria, F. A.; Zhang, W.; van Duin, A. C. T.; Patrito, E. M. Thermal Stability of Organic Monolayers Grafted to Si(111): Insights from ReaxFF Reactive Molecular Dynamics Simulations. *ACS Appl. Mater. Interfaces* **2017**, *9*, 30969–30981.

(36) Evans, D. J.; Holian, B. L. The Nose–Hoover thermostat. *J. Chem. Phys.* **1985**, *83*, 4069–4074.

(37) Stukowski, A. Visualization and analysis of atomistic simulation data with OVITO—the Open Visualization Tool. *Modell. Simul. Mater. Sci. Eng.* **2010**, *18*, 015012.

(38) Jas, G. S.; Wang, Y.; Pauls, S. W.; Johnson, C. K.; Kuczera, K. Influence of temperature and viscosity on anthracene rotational diffusion in organic solvents: Molecular dynamics simulations and fluorescence anisotropy study. *J. Chem. Phys.* **1997**, *107*, 8800–8812.

(39) Lecot, S.; Lavigne, A.; Yang, Z.; Géhin, T.; Botella, C.; Joussemae, V.; Chevrolot, Y.; Phaner-Goutorbe, M.; Yeromonahos, C. Arrangement of Monofunctional Silane Molecules on Silica Surfaces: Influence of Alkyl Chain Length, Head-Group Charge, and Surface Coverage, from Molecular Dynamics Simulations, X-ray Photoelectron Spectroscopy, and Fourier Transform Infrared Spectroscopy. *J. Phys. Chem. C* **2020**, *124*, 20125–20134.

(40) Roscioni, O. M.; Muccioli, L.; Mityashin, A.; Cornil, J.; Zannoni, C. Structural Characterization of Alkylsilane and Fluoroalkylsilane Self-Assembled Monolayers on SiO₂ by Molecular Dynamics Simulations. *J. Phys. Chem. C* **2016**, *120*, 14652–14662.

(41) Ghorai, P. K.; Glotzer, S. C. Molecular Dynamics Simulation Study of Self-Assembled Monolayers of Alkanethiol Surfactants on Spherical Gold Nanoparticles. *J. Phys. Chem. C* **2007**, *111*, 15857–15862.

(42) Aldagari, S.; Hung, A. M.; Shariati, S.; Faisal Kabir, S. K.; Ranka, M.; Bird, R. C.; Fini, E. H. Enhanced sustainability at the bitumen-aggregate interface using organosilane coating technology. *Constr. Build. Mater.* **2022**, *359*, 129500.